

THERMODYNAMIC PROPERTIES OF Co–Pr ALLOYS

V. S. Sudavtsova,^{1,3} M. O. Shevchenko,¹ V. G. Kudin,²
L. O. Romanova,¹ and M. I. Ivanov¹

UDC 536.7;541.122

The mixing enthalpies of the Co–Pr liquid binary alloys are determined by isoperibol calorimetry in the composition ranges $0 < x_{Pr} < 0.23$ and $0.4 < x_{Pr} < 1$ at 1500–1820 K. The thermodynamic properties of the Co–Pr liquid binary alloys are calculated for the entire composition range using the model of ideal associated solutions. The thermodynamic activities of components show negative deviations from the ideal behavior; the mixing enthalpies are characterized by moderate exothermic effects. The minimum mixing enthalpy of melts is -12.0 kJ/mol at $x_{Pr} = 0.46$.

Keywords: thermodynamic properties, cobalt, praseodymium, calorimetry.

INTRODUCTION

Binary compounds of lanthanides with iron and cobalt are used in the manufacture of new permanent magnets and hydrogen storage materials. The knowledge of the thermodynamic properties and phase diagrams of these systems is essential for improving the production of such materials and predicting their stability in operation.

The Co–Pr system has been of continuous research interest. The phase equilibria in Co–Pr alloys were first examined in [1–2]. Nine intermetallics were reported: $\text{Co}_{17}\text{Pr}_2$, Co_5Pr , $\text{Co}_{19}\text{Pr}_5$, Co_7Pr_2 , Co_3Pr , Co_2Pr , $\text{Co}_{1.7}\text{Pr}_2$, $\text{Co}_{\sim 3}\text{Pr}_{\sim 7}$, and CoPr_3 . All these compounds, except for CoPr_3 , melt incongruently. In [3], $\text{Co}_{\sim 3}\text{Pr}_{\sim 7}$ was replaced by Co_2Pr_5 to account for its crystalline structure [4]. The Co–Pr system was later studied in [5]; eight compounds were found: $\text{Co}_{1.7}\text{Pr}_2$ was replaced by Co_3Pr_4 , and Co_2Pr_5 was not revealed (Fig. 1). In addition, congruent melting of $\text{Co}_{17}\text{Pr}_2$ with a eutectic at 7 at.% Pr was assumed in [5], though the as-cast alloy with 7.1% Pr did not show microstructural features peculiar to eutectics. Hence, peritectic melting of $\text{Co}_{17}\text{Pr}_2$ seems to be more likely. The solubility of Pr in Co is no more than 0.03% and can be neglected. Similar information is provided in [6]. It was found in [7, 8] that intermetallic Co_5Pr was unstable at low temperatures and decomposed into $\text{Co}_{17}\text{Pr}_2$ and $\text{Co}_{19}\text{Pr}_5$.

The formation enthalpy of Co_2Pr was determined in [9]; it is -4.4 kJ/mol. The electromotive force method was employed in [10] to examine the Gibbs energy, enthalpy, and entropy of formation for $\text{Co}_{17}\text{Pr}_2$, Co_5Pr , Co_7Pr_2 , Co_3Pr , and Co_2Pr at 973–1073 K. More exothermic formation enthalpies than in [9] were found; in particular, -15.74 kJ/mol for Co_2Pr . Hence, we consider that these data are more correct. The thermodynamic properties of liquid alloys have not been studied so far.

¹Frantsevich Institute for Problems of Materials Science, National Academy of Sciences of Ukraine, Kiev, Ukraine. ²Taras Shevchenko National University, Kiev, Ukraine.

³To whom correspondence should be addressed; e-mail: sud@materials.kiev.ua.

Translated from Poroshkovaya Metallurgiya, Vol. 56, Nos. 1–2 (513), pp. 122–131, 2017. Original article submitted October 1, 2014.

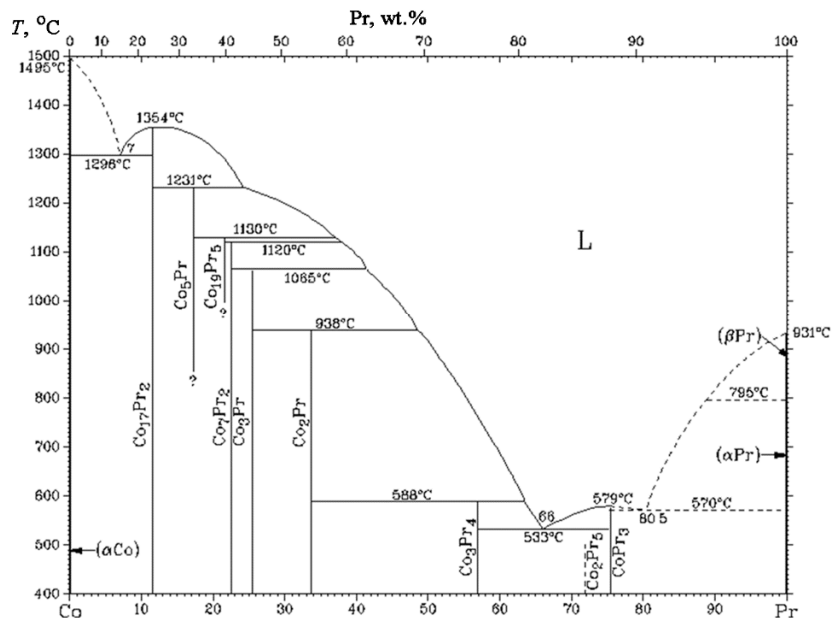


Fig. 1. The Co–Pr phase diagram according to [3] based on [5]

The thermodynamic properties and phase diagram of Co–Pr alloys were described using the Calphad method in [11].

Our objective is to determine the mixing enthalpies of the Co–Pr melts by calorimetry over a wide composition range and then use these results and published data to calculate the thermodynamic properties of the alloys and coordinates of the liquidus lines employing the IAS model.

EXPERIMENTAL PROCEDURE

The experimental procedure is described in [12]. The starting materials were cobalt (99.99%), praseodymium (99.9%), and molybdenum (99.9%). Two experiments in alumina crucibles were performed for cobalt. In one experiment, the initial mass of cobalt was 3160 mg and that of Pr was 10.1–56 mg. In the other experiment, the initial melt contained Co (1074 mg) and Pr (179 mg), to which Co samples (14–23 mg) for calibration and Pr samples (19–30 mg) were added. For praseodymium, also two experiments in molybdenum crucibles were performed. The starting melt contained pure praseodymium (1300–1400 mg), to which Pr samples for calibration (13–30 mg) and Co samples (10–36 mg) were added.

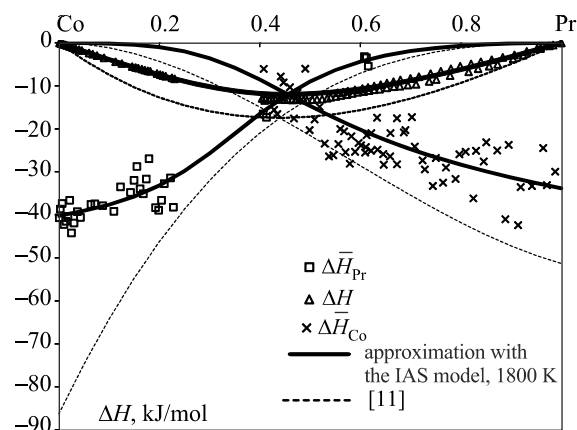


Fig. 2. Partial ($\overline{\Delta H}_{Pr}$, $\overline{\Delta H}_{Co}$) and integral (ΔH) mixing enthalpies of components in the Co–Pr melts experimentally obtained at 1500–1820 K and optimized with the IAS model versus published data

We first determined the mixing enthalpies of the Co–Pr melts over a wide composition range ($0 < x_{\text{Pr}} < 0.23$ and $0.4 < x_{\text{Pr}} < 1$) at 1500–1820 K (Fig. 2). We conducted the only one experiment at 1500 K for the Pr-rich melts, the dissolution rate of some Co samples being insufficient (undissolved residues of the samples were found in the as-cast alloy following the experiment); therefore, some thermal effects are questionable.

The other experiments were performed at 1720–1820 K. Since the experimental error substantially exceeded the contribution of temperature dependence, we processed and optimized all data at 1800 K.

The calorimeter was calibrated against six or seven samples of the metal contained in pure state in the crucible at the beginning of the experiments and against 0.017–0.036 g molybdenum samples. To calculate thermal effects accompanying the dissolution of the samples, we used the heat balance equation:

$$K \int_0^{\tau_{\infty}} (T - T_0) dt = \Delta H_T + n_i \Delta H_{298}^T,$$

where ΔH_{298}^T is the enthalpy of heating 1 mol of the addition from 298 K to the experimental temperature calculated with the equations from [13]; K is the calorimeter heat-exchange coefficient, determined by calibration component A as follows:

$$K = \Delta H_{298}^{T_0}(A) n_A / \int_0^{\tau_{\infty}} (T - T_0) dt;$$

n_i is the amount of the addition, mol; τ_{∞} is the temperature relaxation time in recording the heat-exchange curve; $T - T_0 = \Delta T$ is the temperature difference between the crucible with the melt and isothermal calorimeter shell; t is time.

The partial mixing enthalpies of one component were used to calculate those of the other component by integrating the Gibbs–Duhem equation. The integral mixing enthalpies of the melts were calculated with the equation that holds when concentration of the component i slightly changes from x_i^n to x_i^{n+1} after adding the $(n + 1)$ -th sample:

$$\Delta H^{n+1} = \Delta H^n + \left(\Delta \bar{H}_i^{n+1} - \Delta H^n \right) \left(x_i^{n+1} - x_i^n \right) / \left(1 - x_i^n \right).$$

The experimental data were mutually agreed employing the software based on the ideal associated solution (IAS) model described below.

The measurement errors were determined from root-mean-square deviations of experimental data points of the fitting curves obtained with the IAS model. The composition dependences of the errors were considered to be proportionate to the respective functions (partial or integral mixing enthalpies).

EXPERIMENTAL AND MODELLING RESULTS

Figure 2 summarizes results of the experiments conducted to determine the thermochemical properties of Co–Pr binary melts. For processing of the results obtained (considering all reliable published data on the thermodynamic properties and phase equilibria), we used the IAS model. The success of this model was continuously confirmed when it was used to assess the thermodynamic properties of binary alloys with strong interaction energy between the components, including Eu–Al (Sn, Pd, Pt, Cu, Ag) [14], Al–La [15], Al–Yb [16], and Ce–Si [17]; the main model principles and equations are described in the referenced papers. All these systems consist of lanthanides and elements with greater electronegativity and tend to form clusters whose energy is due to the transfer of electron density from the active metal (donor) to the acceptor element. The Co–Pr system also fits into this group.

To determine the thermodynamic properties, we assume that one to six associates exist in the melt, their number being commonly greater for systems with strong interaction energy between the components. The composition of associates is usually closer to that of compounds formed in solid alloys but not completely the same

since the melts exist at higher temperatures when the entropy contribution is essential. This leads to the simplest groups (AB , A_2B , AB_2), while associates such as A_5B_3 , A_7B_6 , etc. are very unlikely to exist, though the solid alloys show compounds of such composition when the respective crystalline structure is favored in terms of energy. The significant curvature (i.e., the second derivative) of the integral mixing enthalpy near the relevant melt composition is an additional criterion that determines the existence of an associate with specific stoichiometry; the partial mixing enthalpies of the components show significant first derivatives in this region.

The formation enthalpies and entropies of associates ($\Delta_f H^{\text{liq}}$, $\Delta_f S^{\text{liq}}$) are model parameters for the melts; since phase equilibria with solid compounds and pure components are considered as well, the formation enthalpies and entropies of solid phases ($\Delta_f H^{\text{sol}}$, $\Delta_f S^{\text{sol}}$), being independent of temperature, are added. In more complex cases, the Gibbs energy of formation for solid phases cannot be described by a linear temperature dependence. Moreover, homogeneity ranges of solid phases are likely to exist.

If $\Delta_f H_n^{\text{liq}}$ and $\Delta_f S_n^{\text{liq}}$ are known for associates $A_{i_n} B_{j_n}$, the melt equilibrium composition is found by minimization of the function

$$\Delta G = RT \cdot \left(a_A \ln a_A + a_B \ln a_B + \sum_{n=1}^N x_n \left(\frac{\Delta G_n}{RT} + \ln x_n \right) \right) / \left(1 + \sum_{n=1}^N (i_n + j_n - 1) x_n \right),$$

where $\Delta G_n = \Delta_f H_n^{\text{liq}} - T \Delta_f S_n^{\text{liq}}$; $a_A = x_{A_1}$ and $a_B = x_{B_1}$ are the molar fractions of monomers, which are equal to the activities of components in accordance with the model principles; and x_n are the molar fractions of the associates. The standardization conditions are

$$a_A + a_B + \sum_{n=1}^N x_n = 1,$$

$$1 - x_A = x_B = \left(a_B + \sum_{n=1}^N x_n j_n \right) / \left(a_A + a_B + \sum_{n=1}^N x_n (i_n + j_n) \right),$$

where x_A and x_B are the total molar fractions of components in the melt.

TABLE 1. Enthalpies $\Delta_f H$ (kJ/mol) and Entropies $\Delta_f S$ (J/mol/K) of Formation for Associates in the Melts (liq) and Compounds (sol) in the Co–Pr System Optimized with the IAS Model versus Published Data

Compound	IAS model				1073 K [10]		Evaluation [11]	
	$-\Delta_f H^{\text{liq}}$	$-\Delta_f S^{\text{liq}}$	$-\Delta_f H^{\text{sol}}$	$-\Delta_f S^{\text{sol}}$	$-\Delta_f H^{\text{sol}}$	$-\Delta_f S^{\text{sol}}$	$-\Delta_f H^{\text{sol}}$	$-\Delta_f S^{\text{sol}}$
Co ₁₇ Pr ₂			8.9	1.8	5.91	-0.85	6.76 (8.31*)	0.67 (2.20)
Co ₅ Pr			11.6	1.7	8.17	-1.46	10.55 (13.15)	1.58 (4.89)
Co ₇ Pr ₂			16.2	3.9	12.47	0.48	16.08 (17.19)	4.56 (6.82)
Co ₃ Pr			17.4	4.3	13.96	1.05	16.14 (17.09)	4.25 (7.51)
Co ₂ Pr	16.1	5.6	18.2	4.3	15.74	1.58	15.23 (15.38)	2.97 (6.69)
CoPr	22.1	7.3						
Co ₃ Pr ₄			13.7	2.8			10.50	0.34
CoPr ₃			8.9	1.6			6.84	-0.36

* The paper [11] accounts for the magnetic contributions to the thermodynamic properties of compounds in the Co–Pr system. The first value is valid for near-liquidus temperatures ($T \gg T_C$, where T_C is Curie temperature) and the second value (in parentheses) for $T \ll T_C$.

When minimum ΔG and associated a_A , a_B , and x_n ($n=1\dots N$) are found, other thermodynamic functions can be calculated, for example:

$$\Delta H = \left(\sum_{n=1}^N \Delta_f H_n \cdot x_n \right) / \left(1 + \sum_{n=1}^N (i_n + j_n - 1) x_n \right).$$

To calculate the thermodynamic properties from parameters $\Delta_f H_n^{\text{liq}}$ and $\Delta_f S_n^{\text{liq}}$ and optimize these parameters to approximate the thermodynamic properties to experimental data to the extent possible, we developed our own programs.

For modeling, we assumed that two associates with the simplest composition (Co_2Pr and CoPr) existed in the melts. It should be noted that we did not consider $\text{Co}_{19}\text{Pr}_5$ (with composition very close to Co_7Pr_2 and with a very narrow and thus negligible melt equilibrium range) and Co_2Pr_5 in our modelling. The model parameters are summarized in Table 1 and in Figs. 3 and 4 versus published data.

The integral and partial mixing enthalpies and entropies of the Co–Pr melts optimized with the IAS model at 1800 K (Table 2) can be fitted to the following polynomial dependences:

$$\Delta H = x_{\text{Pr}}(1 - x_{\text{Pr}})(-39 - 61.97x_{\text{Pr}} + 117x_{\text{Pr}}^2 - 49.57x_{\text{Pr}}^3);$$

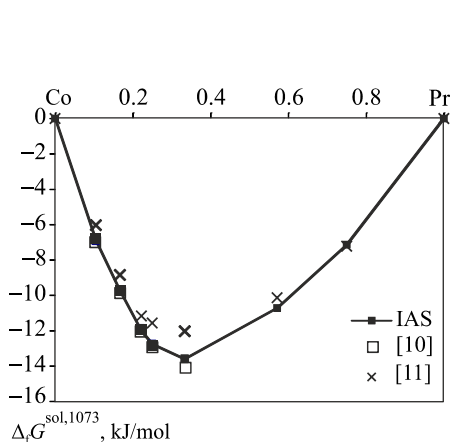


Fig. 3. Gibbs energies of formation for Co–Pr intermetallics at 1073 K found with the emf method [10] and according to our IAS model and [11]

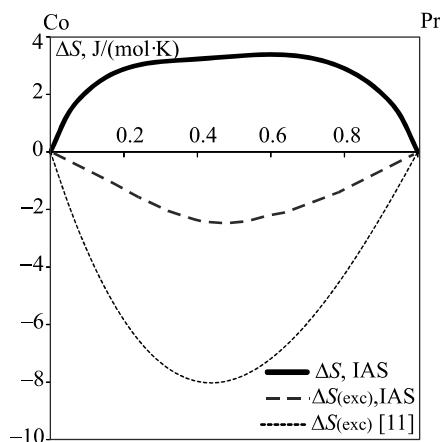


Fig. 4. Entropies and excess mixing entropies of the Co–Pr melts at 1800 K according to the IAS model and [11]

TABLE 2. Integral and Partial Mixing Enthalpies for Rounded Concentrations of Components in the Co–Pr Melts at 1800 K, kJ/mol

x_{Pr}	$-\Delta H$	$-\Delta \bar{H}_{\text{Co}}$	$-\Delta \bar{H}_{\text{Pr}}$
0	0	0	40.2 ± 3.5
0.1	3.9 ± 0.4	0.2 ± 0.0	37.6 ± 3.3
0.2	7.4 ± 0.8	1.0 ± 0.2	33.2 ± 2.9
0.3	10.2 ± 1.1	3.6 ± 0.8	25.7 ± 2.3
0.4	11.7 ± 1.2	8.6 ± 1.9	16.5 ± 1.5
0.5	11.8 ± 1.2	14.7 ± 3.3	9.0 ± 0.8
0.6	10.7 ± 1.1	20.2 ± 4.5	4.4 ± 0.4
0.7	8.8 ± 0.9	24.7 ± 5.5	1.9 ± 0.2
0.8	6.2 ± 0.6	28.3 ± 6.4	0.7 ± 0.1
0.9	3.3 ± 0.3	31.3 ± 7.0	0.1 ± 0.0
1	0	33.8 ± 7.6	0

$$\begin{aligned} \overline{\Delta H}_{\text{Co}} &= x_{\text{Pr}}^2(22.97 - 357.9x_{\text{Pr}} + 499.7x_{\text{Pr}}^2 - 198.3x_{\text{Pr}}^3); \\ \overline{\Delta H}_{\text{Pr}} &= (1 - x_{\text{Pr}})^2(-39 - 123.9x_{\text{Pr}} + 351x_{\text{Pr}}^2 - 198.3x_{\text{Pr}}^3); \\ \Delta S^{\text{ex}} &= x_{\text{Pr}}(1 - x_{\text{Pr}})(-4.88 - 23.9x_{\text{Pr}} + 35.96x_{\text{Pr}}^2 - 13.71x_{\text{Pr}}^3); \\ \overline{\Delta S}_{\text{Co}}^{\text{ex}} &= x_{\text{Pr}}^2(19.02 - 119.7x_{\text{Pr}} + 149x_{\text{Pr}}^2 - 54.84x_{\text{Pr}}^3); \\ \overline{\Delta S}_{\text{Pr}}^{\text{ex}} &= (1 - x_{\text{Pr}})^2(-4.88 - 47.8x_{\text{Pr}} + 107.9x_{\text{Pr}}^2 - 54.84x_{\text{Pr}}^3). \end{aligned}$$

These dependences can be used further to calculate the thermodynamic properties and phase diagrams of multicomponent systems based on the bounding Co–Pr system.

Figures 5–7 show the thermodynamic properties of the Co–Pr melts that correspond to the optimized IAS model.

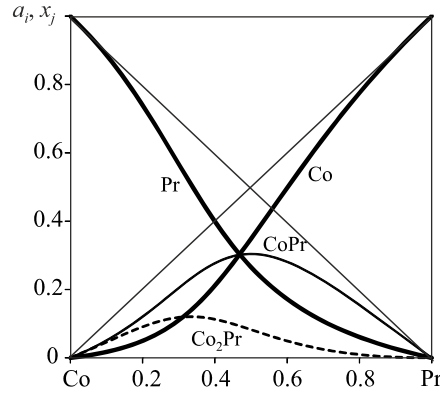


Fig. 5. Activities of components (a_i) and molar fractions of associates (x_j) in the Co–Pr melts at 1800 K calculated with the IAS model

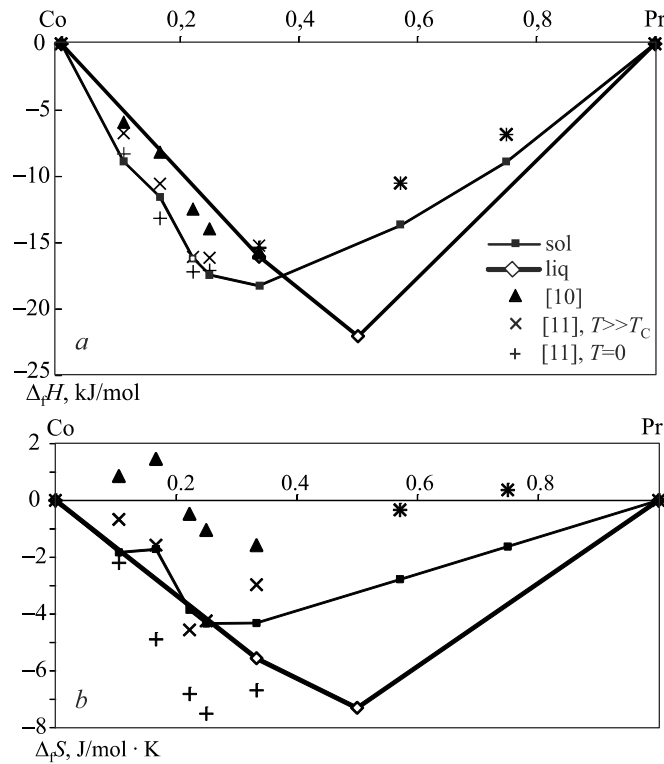


Fig. 6. Enthalpies (a) and entropies (b) of formation for intermetallics (sol) and associates (liq) in the Co–Pr melts according to our IAS model and [11] (indicated separately for high and low temperatures for ferromagnetic compounds) and found with the emf method at 973–1073 K [10]

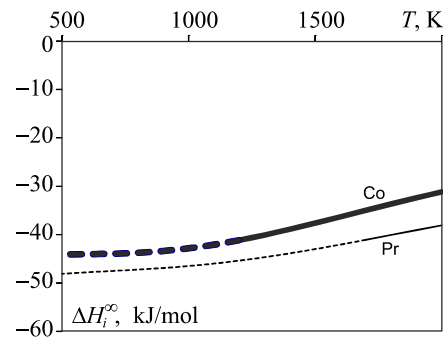


Fig. 7. Temperature dependences of the first partial mixing enthalpies of components in liquid or overcooled (dashed line) Co–Pr melts according to the IAS model

Hence, the activities of components show moderate negative deviations from the Raoult law; the predominant associate is CoPr, and small asymmetry of the thermodynamic properties of components is attributed to the formation of Co₂Pr associate.

DISCUSSION OF RESULTS

The thermal mixing effects for the melts are moderately exothermic ($\Delta H_{\min} = -12.0 \pm 1.2$ at $x_{\text{Pr}} = 0.46$; $\overline{\Delta H}_{\text{Pr}}^{\infty} = -40.2 \pm 3.5$; $\overline{\Delta H}_{\text{Co}}^{\infty} = -33.8 \pm 7.6$ kJ/mol). This agrees with the results reported in [11] only at a qualitative level; they turned out to be 1.5–2 times overestimated.

Figure 6 shows that the formation enthalpies and entropies that we calculated for Co–Pr intermetallics are more negative than those reported in [10] and [11]. Nevertheless, Fig. 3 demonstrates that these deviations are compensated for in transfer to the formation Gibbs energies of compounds, which is the primary information obtained in [11] with the electromotive force method, while the enthalpies and entropies reported in the referenced papers were found by electromotive force differentiation (ΔG) with respect to temperature, which could not be sufficiently accurate because of a narrow temperature range. Therefore, our data are reliable.

The excess mixing entropies of the Co–Pr melts are small negative values, being one-third the results reported in [11], and total mixing entropies are small positive values. The difference from [11] again compensates for similar difference with the mixing enthalpies; hence, our Gibbs mixing energies of the melts at 1000–1800 K and those reported in [11] are very close.

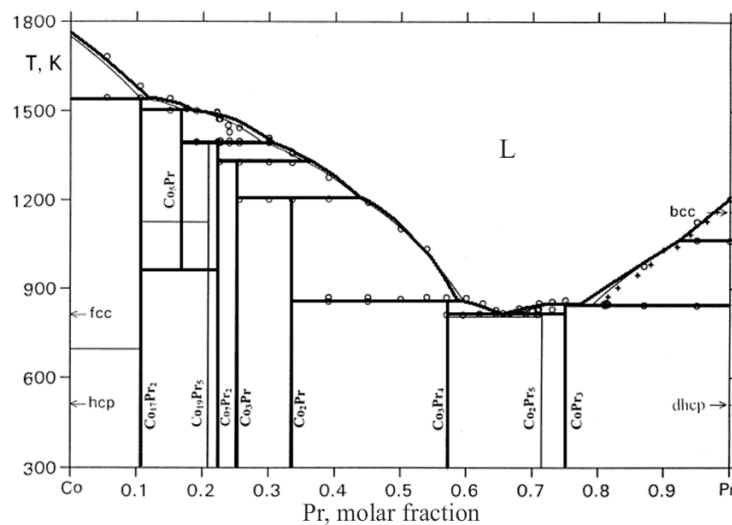


Fig. 8. The Co–Pr phase diagram according to our IAS model and published data: lines denote data from [11] and points from [2]

Figure 8 shows that our liquidus line of the Co–Pr phase diagram agrees well with reliable experimental data [2] (at least not less well than [11] for $0 < x_{\text{Pr}} < 0.8$ and somewhat worse for $0.8 < x_{\text{Pr}} < 1$).

The above-stated information, as well as good agreement of our parameters with those evaluated in [11], confirms that all our experimental and calculated data are reliable.

CONCLUSIONS

We have used the experimental mixing enthalpies that we obtained for Co–Pr binary melts for the first time to construct a thermodynamic model of these alloys over a wide temperature range that agrees with all reliable published data.

This model continues the other studies focusing on the thermodynamics and phase equilibria for these alloys.

REFERENCES

1. A. E. Ray and G. I. Hoffer, “Phase diagrams for the Ce–Co, Pr–Co, and Nd–Co alloy systems,” in: *Proc. Eighth Rare Earth Research Conference*, Reno, Nevada (1970), p. 524.
2. A. E. Ray, A. T. Biermann, R. S. Harmer, and J. E. Davison, “Revision of the phase diagrams of the cerium–cobalt, praseodymium–cobalt, and neodymium–cobalt binary systems,” *Cobalt*, **4**, 103–106 (1973).
3. T. B. Massalski, P. R. Subramanian, H. Okamoto, and L. Kacprzak, *Binary Alloy Phase Diagrams*, 2nd ed., ASM International, Materials Park, Ohio (1990).
4. J. M. Moreau and D. Paccard, “The monoclinic crystal structure of R_5Co_2 (R = Pr, Nd, Sm) with the Mn_5C_2 structure type,” *Acta Crystallogr.*, **B32**, 1654–1656 (1976).
5. C. H. Wu, Y. C. Chuang, X. M. Jin, and X. H. Guan, “Re-investigation of the Pr–Co binary system,” *Z. Metallkd.*, **83**, 32–34 (1992).
6. H. Okamoto, “Co–Pr (cobalt–praseodymium),” *J. Phase Equilib.*, **13**, 675–676 (1992).
7. Y. C. Chuang, C. H. Wu, S. C. Chang, et al., “Effect of heat treatment on the microstructure and coercivity of PrCo_5 ,” *J. Less-Common Met.*, **125**, 25–28 (1986).
8. K. H. J. Buschow, “Note on the stability of rare earth–cobalt compounds with CaCu_5 structure,” *J. Less-Common Met.*, **29**, 283 (1972).
9. S. S. Deodhar and P. J. Ficalora, “A study of the reaction kinetics for the formation of rare earth-transition metal laves compounds,” *Metall. Trans.*, **6A**, 1909–1914 (1975).
10. S. Bär and H.-J. Schaller, “Thermodynamic properties of cobalt–praseodymium alloys,” *Thermochim. Acta*, **314**, 131–136 (1998).
11. Z. Du, D. Wang, and W. Zhang, “Thermodynamic assessment of the Co–Pr, Er–Ni, and Ni–Pr systems,” *J. Alloys Compd.*, **284**, 206–212 (1999).
12. M. Ivanov, V. Berezutski, and N. Usenko, “Mixing enthalpies in liquid alloys of manganese with the lanthanides,” *J. Mater. Res.*, **102**, 277 (2011).
13. A. T. Dinsdale, “SGTE data for pure elements,” *Calphad*, **15**, No. 4, 319 (1991).
14. M. I. Ivanov, V. V. Berezutskii, M. O. Shevchenko, et al., “Interaction in the europium-containing alloys,” *Dop. Nats. Acad. Nauk Ukrainy*, No. 8, 90–99 (2013).
15. V. G. Kudin, M. A. Shevchenko, I. V. Mateiko, and V. S. Sudavtsova, “Thermodynamic properties of Al–La melts,” *Zh. Fiz. Khim.*, **87**, No. 3, 364–370 (2013).
16. V. S. Sudavtsova, M. I. Ivanov, V. V. Berezutskii, et al., “Mixing enthalpy of Al–Yb melts,” *Zh. Fiz. Khim.*, **86**, No. 8, 1311–1315 (2012).
17. M. A. Shevchenko, V. G. Kudin, N. G. Kobylinskaya, and V. S. Sudavtsova, “Thermodynamic properties and phase diagram of the Ce–Si system,” *Ukr. Khim. Zh.*, **78**, No. 6, 96–102 (2012).